



Quantum impurity model for two-stage multipolar ordering and Fermi surface reconstructionDaniel J. Schultz ^{*}, SangEun Han ^{*}, and Yong Baek Kim*Department of Physics, University of Toronto, Toronto, Ontario M5S 1A7, Canada*

(Received 4 May 2023; revised 19 July 2023; accepted 25 July 2023; published 8 August 2023)

Classification and understanding of quantum phase transitions and critical phenomena in itinerant electron systems are outstanding questions in quantum materials research. Recent experiments on heavy fermion systems with higher-rank multipolar local moments provide a new platform to study such questions. In particular, experiments on $\text{Ce}_3\text{Pd}_{20}(\text{Si}, \text{Ge})_6$ show novel quantum critical behaviors via two consecutive magnetic field-driven quantum phase transitions. At each transition, the derivative of the Hall resistivity jumps discontinuously, which was attributed to sequential Fermi surface reconstructions. Motivated by this discovery, we consider an effective quantum impurity model of itinerant electrons coupled to local dipolar, quadrupolar, and octupolar moments arising from Ce^{3+} ions. Using renormalization group analyses, we demonstrate that two-stage multipolar ordering and Fermi surface reconstruction arise depending on which multipolar moments participate in the Fermi surface and which other moments are decoupled via Kondo destruction.

DOI: [10.1103/PhysRevB.108.L060401](https://doi.org/10.1103/PhysRevB.108.L060401)

Introduction. Experimental work on rare-earth metallic systems has shown a wide variety of quantum phases of matter and novel quantum phase transitions (QPTs). In some systems, f electrons give rise to multipolar moments, and these moments couple to itinerant conduction electrons; this situation is described by a multipolar Kondo lattice model. Since we have a large number of degrees of freedom and constraining crystal field symmetries, Kondo couplings become highly anisotropic in contrast to the conventional dipolar Kondo lattice model. Hence we can expect to find more diverse novel quantum phenomena such as the emergence of the new types of Kondo phases, RKKY mediated multipolar ordered phases [1,2], and novel quantum criticality from the competition between them [3–14]. Many of these phenomena are not yet well understood, and researchers face ongoing challenges to theoretically describe and experimentally detect these multipolar quantum phases [15–32].

One class of metallic systems, which contains multipolar moments is $\text{Ce}_3\text{Pd}_{20}(\text{Si}, \text{Ge})_6$. Here, the magnetically active Ce^{3+} ions ($4f^1$ configuration) are surrounded by a tetrahedral crystal field, which constrains the Ce^{3+} ground state to be a fourfold degenerate quartet [33–35]. The four states consist of two degenerate Kramers doublets, and support a large number of the multipolar moments (see Table I) [36].

Experimental studies on $\text{Ce}_3\text{Pd}_{20}\text{Si}_6$ in particular show novel quantum critical behaviors corresponding to two consecutive field-induced QPTs [34,37–41]. At zero magnetic field, the system exhibits coexisting antiferromagnetic and antiferroquadrupolar order, and by increasing the external magnetic field along [001], the antiferromagnetic order disappears but the antiferroquadrupolar order remains. Upon increasing the field further, the system arrives at another phase

that has not been clearly identified yet. Interestingly, the experiment observed that the derivative of the Hall resistivity with respect to magnetic field, when extrapolated to zero-temperature, jumps at both phase transitions. These jumps indicate sequential Fermi surface reconstruction [42–49].

In this work, we study a theoretical model for the existence of such a two-stage QPT and extract the types of magnetic order in the context of experiments on $\text{Ce}_3\text{Pd}_{20}\text{Si}_6$, as well as suggest experimental signatures of the quantum critical points. For simplicity, we construct a multipolar Bose-Fermi Kondo model of 15 multipolar moments of the Ce^{3+} quartet coupled to both p -wave conduction electrons and a dynamical bosonic bath representing RKKY interactions [50–55]. Despite now being a local approximation of the Kondo lattice in the form of an impurity model in the spirit of dynamical mean-field theory, the fact that the impurity is coupled to a bosonic bath via Bose-Kondo couplings means that magnetic fluctuations due to other sites are included in addition to the usual Fermi-Kondo effect with the fermionic (conduction electrons) bath. This model therefore facilitates a study of the competition between the Kondo effect and magnetic ordering. We use the renormalization group approach to determine the permissible types of magnetic order and Kondo destruction pathways purely on the basis of local symmetry. Specifically, we examine which local moments participate in the Fermi surface and which local moments are ordered and decouple from the conduction electrons in each part of the zero temperature phase diagram. We then discuss experimental consequences of our findings.

Models. As mentioned in the introduction, our effective model for this system consists of a single local multipolar moment coupled to conduction electrons and a dynamical bosonic bath representing RKKY magnetic fluctuations. To construct the model, we consider the local symmetry at the Ce^{3+} ion site in $\text{Ce}_3\text{Pd}_{20}(\text{Si}, \text{Ge})_6$. For this family of materials, there are two crystallographically distinct sites for

^{*}These authors contributed equally to this work.

TABLE I. Multipolar moments, J_x, J_y, J_z are $J = 5/2$ operators. The overline notation means full symmetrization. For example $\overline{AB} = AB + BA$, $\overline{A^2B} = A^2B + ABA + BA^2$, and $\overline{ABC} = ABC + ACB + BAC + BCA + CAB + CBA$. The irrep column denotes irreducible representations of T_d , and the Stevens column contains Stevens operators. The + subscripts on the T_2 moments denote the time-reversal even/odd nature of the moments for quadrupole/octupoles. We do not include a + label if there is no ambiguity. In the moment column, we indicate if the moment is dipolar (D), quadrupolar (Q), or octupolar (O).

Irrep	Stevens	In terms of J_x, J_y, J_z	Moment
T_1	J_x	J_x	D
T_1	J_y	J_y	D
T_1	J_z	J_z	D
E	O_{22}	$\frac{\sqrt{3}}{2}(J_x^2 - J_y^2)$	Q
E	O_{20}	$\frac{1}{2}(3J_z^2 - J^2)$	Q
T_{2+}	O_{yz}	$\frac{\sqrt{3}}{2}J_yJ_z$	Q
T_{2+}	O_{zx}	$\frac{\sqrt{3}}{2}J_zJ_x$	Q
T_{2+}	O_{xy}	$\frac{\sqrt{3}}{2}J_xJ_y$	Q
A_2	\mathcal{T}_{xyz}	$\frac{\sqrt{15}}{6}J_xJ_yJ_z$	O
T_1	\mathcal{T}_x^α	$\frac{1}{2}(2J_x^3 - \overline{J_xJ_y^2} - \overline{J_z^2J_x})$	O
T_1	\mathcal{T}_y^α	$\frac{1}{2}(2J_y^3 - \overline{J_yJ_z^2} - \overline{J_x^2J_y})$	O
T_1	\mathcal{T}_z^α	$\frac{1}{2}(2J_z^3 - \overline{J_zJ_x^2} - \overline{J_y^2J_z})$	O
T_{2-}	\mathcal{T}_x^β	$\frac{\sqrt{15}}{6}(\overline{J_xJ_y^2} - \overline{J_z^2J_x})$	O
T_{2-}	\mathcal{T}_y^β	$\frac{\sqrt{15}}{6}(\overline{J_yJ_z^2} - \overline{J_x^2J_y})$	O
T_{2-}	\mathcal{T}_z^β	$\frac{\sqrt{15}}{6}(\overline{J_zJ_x^2} - \overline{J_y^2J_z})$	O

Ce ions: the 4a and 8c sites [40,56]. The magnetically active Ce ions occupy the 8c sites and are surrounded by a Pd_{16} cage, which has tetrahedral T_d symmetry. We construct the Bose-Fermi Kondo model for the system to include all symmetry-allowed interactions. To find such symmetry-allowed interactions, we list the transformations of constituent elements in the model under the tetrahedral group T_d and time reversal in Supplemental Material [57].

The degenerate ground states of an ion in a vacuum can be described by an effective higher-spin system through Hund's rules. For the case of a Ce^{3+} ion, it has a $4f^1$ configuration and resulting $J = 5/2$ moment. In the presence of the T_d CEF, the 6 degenerate states split and a Γ_8 quartet ground state is formed. The states of this quartet are listed in Supplemental Material [57]. Since there are four degenerate ground states, numerous multipolar moments can be formed; in particular we have three dipolar, five quadrupolar, and seven octupolar moments [36], which are tabulated in Table I. In the table they are classified by time reversal and by irreps of T_d . The details of how the multipolar operators are constructed from the quartet states, as well as how to represent the multipolar operators by Abrikosov pseudofermions (which is required for the renormalization group analysis), are in the Supplemental Material [57].

We now turn to the Fermi-Kondo model, where we couple the local moments to conduction electrons. The conduction

electron wave functions are considered to be molecular orbitals centered on the Ce ion and constructed from electrons hopping on the Pd_{16} cage. The resulting wave functions are classifiable according to irreducible representations of T_d . We construct a model of three degenerate bands of conduction electrons, made up of Wannier functions, which lie in the T_2 irrep. of T_d . We may use p -wave $\{x, y, z\}$ orbitals, or d -wave T_2 $\{yz, zx, xy\}$ orbitals; the results are identical with either choice and we use p -wave in this work. We assume a constant density of states for the conduction electrons, and couple them to the local moment in the maximal way allowed by symmetry; this leads to 15 coupling constants [57] (this is unrelated to the fact that there are 15 multipolar moments).

Lastly, we construct the Bose-Kondo part of the model, where the local moments are coupled to the fluctuating bosonic bath. In the case of a lattice of multipolar moments, the spin bilinear RKKY interaction is induced by the conduction electrons. As mentioned before, we capture such an interaction in the Bose-Fermi Kondo model by replacing it with a bosonic bath, which can be thought of as a dynamical Weiss mean field. The Bose-Kondo couplings are determined by the number of independent irreps., so we have 6 bosonic couplings because two of the four irreps are counted twice, namely T_1 and T_2 (see Table I). The details of deriving the symmetry-allowed bosonic couplings for the model are given in Supplemental Material [57]. The Hamiltonian for the kinetic part of the bosonic bath is shown as $H_0^B = \sum_{i,\mathbf{k}} \Omega_{\mathbf{k}} \phi_{\mathbf{k}}^{i\dagger} \phi_{\mathbf{k}}^i$, where we assume that all flavors are degenerate for simplicity. The index $i = 1, \dots, 15$ runs over all bosonic baths, and $\Omega_{\mathbf{k}}$ is the dispersion of the bosonic fields. In order to perform the RG analysis, we set up an ϵ expansion, where ϵ controls the sublinearity of the spectral function of the bosonic bath:

$$\sum_{\mathbf{k}} [\delta(\omega - \Omega_{\mathbf{k}}) - \delta(\omega + \Omega_{\mathbf{k}})] = \frac{N_1^2}{2} |\omega|^{1-\epsilon} \text{sgn}(\omega). \quad (1)$$

Because we assumed that all flavors of the bosonic bath were degenerate, they also all have the same ϵ controlling their densities of states.

As a result, by adding the Fermi-Kondo and Bose-Kondo interactions, we construct the full Bose-Fermi Kondo model, which yields a model with a grand total of $15 + 6 = 21$ coupling constants, and we compute the full beta functions [57,58].

Fixed points of the Bose-Fermi Kondo model and two-stage Kondo destruction QPT. From the beta functions we calculate, we can find a number of stable fixed points, but not all are physically important. In the following, we will discuss three stable fixed points, F , B , P , and two critical points, C_{FP} and C_{PB} , between them, and how they are connected by the two-stage Kondo destruction QPT.

The first type of stable fixed point is a Fermi-Kondo fixed point, whose representative is F . This type of phase has local moments hybridized into the Fermi surface and hence has the largest Fermi surface. It is paramagnetic, may be Fermi or non-Fermi liquid [59–63], and can be found within the Fermi-Kondo models. These points have nonzero Fermi-Kondo couplings, while their Bose-Kondo couplings are all zero. For the fixed point F in particular, its fixed point

Hamiltonian H_F corresponds to a 6-generator truncated $SU(4)$ fixed point [64], and thus H_F can be written as follows:

$$H_F = \frac{1}{2} \sum_{\rho, \tau=1}^4 \tilde{\psi}_\rho^\dagger [(\sigma^0 \otimes \vec{\sigma})_{\rho\tau} \cdot (Q^x, O^y, Q^z)] \tilde{\psi}_\tau + \sum_{\rho, \tau=1}^2 \psi_\rho^\dagger [\vec{\sigma}_{\rho\tau} \cdot (D^x, D^y, D^z)] \psi_\tau, \quad (2)$$

where $\vec{\sigma} = (\sigma^x, \sigma^y, \sigma^z)$, $\tilde{\psi}$ and ψ are four- and two-component spinors, respectively (see Supplemental Material for the relationship between these new electrons and the original p -wave conduction electrons via a change of basis [21,22,57]). Here, $\{Q^x, O^y, Q^z\} \sim \{\mathcal{O}_{22}, \mathcal{T}_{xyz}, \mathcal{O}_{20}\}$, and $D^{x,y,z} \sim \{J_{x,y,z}\}$. Each set of three multipolar moments satisfies an $SU(2)$ algebra, and the two $SU(2)$ algebras are mutually commuting. Although the two components commute and thus appear decoupled, the leading irrelevant operator does not commute with either the two-channel or one-channel component, which means that they are coupled at any nonzero distance from the fixed point. This fixed point Hamiltonian has twofold degenerate ground states in the strong coupling limit [65,66], so the IR fixed point is valid and likely shows non-Fermi liquid behavior [59–61,63,65,66].

Second, there are the Bose-Kondo fixed points, whose representative is B . These phases have all local moments decoupled from the Fermi surface, and hence have the smallest Fermi surface. These points have nonzero Bose-Kondo couplings, while their Fermi-Kondo couplings are all zero. It means that they are magnetically ordered phases, and can be found within the Bose-Kondo model. In particular, the fixed point B is a multipolar ordered fixed point that has quadrupolar ordering and dipolar ordering with E and T_1 irreps, respectively.

Third, we find a (stable) partially Kondo-destroyed fixed point P . For a general partially Kondo-destroyed point, the multipolar moments are coupled to bosonic baths as well as conduction electrons, so some local moments are absorbed into the Fermi surface (and behave paramagnetically), while others decouple from the Fermi surface and magnetically order. This is only possible due to the large number of local states. In the case of P , the dipolar local moments are absorbed into the Fermi surface whereas the quadrupolar moments undergo magnetic ordering, so this point has a partially shrunk Fermi surface. Note that more details of the fixed points are given in Supplemental Material [57].

Furthermore, we find critical points C_{FP} between F and P , and C_{BP} between B and P . These critical points and stable fixed points are connected by the path of QPTs, $F \leftarrow C_{FP} \rightarrow P \leftarrow C_{BP} \rightarrow B$, represented pictorially in Fig. 1. The physical interpretation is as follows.

At F , as mentioned before, the system is paramagnetic with a large Fermi surface due to Kondo hybridization by one- and two-channel Kondo interactions and absence of Bose-Kondo coupling. When we pass through C_{FP} from F to P , the two-channel Kondo interaction vanishes, so the quadrupolar and octupolar moments are decoupled from the conduction electrons. During this, the quadrupolar Kondo coupling induces

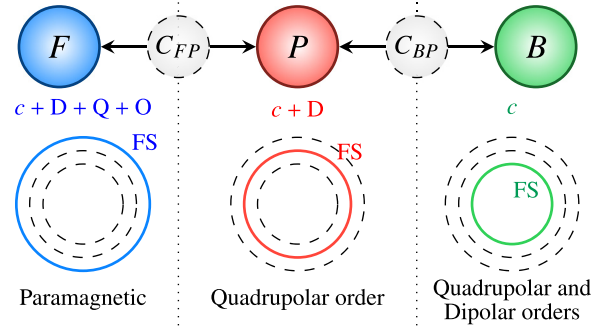


FIG. 1. A schematic diagram for QPT with two-stage Kondo destruction. F , P , and B stand for the fermionic Kondo, partially Kondo destroyed, and magnetically ordered phases, respectively. The second row stands for which degrees of freedom participate in the formation of the Fermi surface. c , D , Q , and O mean conduction electrons, dipolar, quadrupolar and octupolar moments, respectively. The circles in the third row show the schematic size difference of the Fermi surface between each phase depending on how many degrees of freedom participated in the formation of the Fermi surface. The last row means the multipolar ordering at each phase.

nonzero Bose-Kondo coupling for the quadrupolar moments, so we can reach P . At P , since the conduction electrons decouple from the quadrupolar and octupolar moments, the Kondo effect is partially destroyed, but we still have nonzero Kondo couplings with dipolar moments. This corresponds to the Fermi surface shrinking one time, so it has a medium size of the Fermi surface. Furthermore, the decoupled quadrupolar moments order, so it has the quadrupolar order parameters $\sim \{J_x^2 - J_y^2, 3J_z^2 - J^2\}$. Next, when we pass through C_{BP} between P and B , the remaining (dipolar) Kondo hybridization vanishes and thereby induces a nonzero Bose-Kondo coupling for the dipolar moments. This corresponds to a second shrinking of the Fermi surface, as well as magnetic ordering of the dipolar moments. At B , since all the Kondo couplings are zero, the Kondo effect is completely destroyed, and it has a small Fermi surface; the full picture of going from F to B is therefore two-stage Kondo destruction (Fig. 1). Moreover, at B , we have coexistence between quadrupolar ordering and dipolar ordering. The two-stage Kondo destruction QPT is consistent with experiment in the sense that the type of ordering we find matches the observed order parameters. Furthermore, the jump in the derivative of the Hall resistivity is consistent with the Kondo destruction phase transitions we have found. We note that, strictly speaking, the symmetry breaking character of the external magnetic field would modify the analysis, but we have neglected it for simplicity. Note that the RG flow diagrams between the stable fixed points and critical points are presented in the Supplemental Material [57].

Ultrasound measurement of multipolar susceptibility. In addition to the qualitative signature of Fermi surface reconstruction, the multipolar susceptibility exponent can be used to quantitatively identify the fixed points. The multipolar susceptibility is defined by $\chi_i(\tau) = \langle T_\tau S^i(\tau) S^i(0) \rangle \sim (\tau_0/|\tau|)^\gamma$, where S^i is the multipolar moment, γ_i is the multipolar susceptibility exponent, i is an index for the irrep, τ is imaginary time, and $\tau \gg \tau_0$ with the cutoff $\tau_0 = 1/\Lambda \sim 1/\mu$. We label the spin operators by irrep. because any representative from

the irrep yields the same result. From the beta functions, we can compute the multipolar susceptibility exponent [57]. The resulting susceptibility exponents γ_i are presented in Supplemental Material [57]. By assuming that the multipolar moments are primary fields with conformal dimension $\gamma_i/2$, the finite temperature scaling of the multipolar susceptibility is given by [54,67]

$$\chi_i'(\omega, T) \sim \begin{cases} T^{\gamma_i-1} \left(1 + C_{\text{ReI}} \left(\frac{\omega}{T}\right)^2\right), & |\omega/T| \ll 1, \\ \omega^{\gamma_i-1}, & |\omega/T| \gg 1, \end{cases} \quad (3)$$

$$\chi_i''(\omega, T) \sim \begin{cases} T^{\gamma_i-1} \left(\frac{\omega}{T}\right), & |\omega/T| \ll 1, \\ \omega^{\gamma_i-1}, & |\omega/T| \gg 1, \end{cases} \quad (4)$$

where $\chi_i(\omega, T) = \chi_i'(\omega, T) + i\chi_i''(\omega, T)$ and C_{ReI} is a real constant. Although the dipolar susceptibilities can be detected by conventional techniques, the purely multipolar susceptibilities require elastic measurements. One way to achieve this is through ultrasound experiments. The symmetry-allowed free energy produces a linear coupling between strain and quadrupolar moments, which facilitates a relationship between elastic constants and quadrupolar susceptibilities. Furthermore, in the presence of an external magnetic field, a product of magnetic field and strain couples linearly to octupolar moments, adding octupolar susceptibility corrections to the elastic constants (see the Supplemental Material for details on how this coupling arises through symmetry considerations [57]). Then, the resulting renormalized elastic constants in the presence of a small magnetic field $\mathbf{h} = (0, 0, h_z)$ are then given by second-order perturbation theory as [15,67,68]:

$$C_{11} - C_{12} = C_{11}^0 - C_{12}^0 - s_E^2 \chi'_{Q_E} - 2s_-^2 h_z^2 \chi'_{O_2}, \quad (5)$$

$$C_{44} = C_{44}^0 - s_+^2 \chi'_{Q_2} - s_A^2 h_z^2 \chi'_{O_A}, \quad (6)$$

where C_{mn}^0 and C_{mn} are the bare and renormalized elastic constants, and $s_{E,A,\pm}$ are the coupling strengths between multipolar moments and the elastic tensors/external magnetic field. χ'_{Q_E} , χ'_{Q_2} , χ'_{O_2} , χ'_{O_A} are the multipolar susceptibilities for quadrupolar moments in E and T_{2+} irreps, and octupolar moments in T_{2-} and A irreps., respectively. We see that the multipolar susceptibilities χ'_{Q_E} and χ'_{Q_2} can both be measured without an external magnetic field. Once these are determined, the susceptibilities χ'_{O_A} and χ'_{O_-} can then be found. In the case of the dipolar susceptibilities, they couple to the magnetic field linearly, and can be measured by conventional magnetic susceptibility probes such as neutron scattering.

Discussions. In this work, we provided a detailed perturbative renormalization group analysis of the Bose-Fermi Kondo model describing a quartet of local states from $\text{Ce}_3\text{Pd}_{20}(\text{Si, Ge})_6$ [36] coupled to three bands of p -wave conduction electrons. The primary result we find is a two-stage Kondo destruction pair of QPT wherein the Fermi surface shrinks twice as local moments decouple from the Fermi surface and undergo magnetic ordering. The phase with smallest Fermi surface is particularly relevant to recent experiments, and exhibits the coexistence of quadrupolar $\{J_x^2 - J_y^2, 3J_z^2 - J^2\}$ and dipolar $\{J_{x,y,z}\}$ order. This is similar to the low-

temperature and zero magnetic field phase of $\text{Ce}_3\text{Pd}_{20}\text{Si}_6$, which has coexistence of antiferromagnetic $\{J_z\}$ and antiferroquadrupolar $\{3J_z^2 - J^2\}$ orders [39,41,46].

Connected to this magnetically ordered phase is a partially Kondo-destroyed phase wherein the dipolar moments hybridize with and enlarge the Fermi surface, whereas the quadrupolar moments remain ordered and decoupled from the conduction electrons. This partially Kondo-destroyed phase is potentially related to the quadrupolar ordered phase observed in the experiment at low temperatures for magnetic fields between 1T and 2T [40]. Our results show a further phase transition to a paramagnetic phase, where the quadrupolar moments also get hybridized with the Fermi surface and enlarge it a second time. Interestingly, all three of these phases are also observed experimentally at zero magnetic field as a function of temperature; indeed the paramagnetic F phase we calculate could be the experimentally observed paramagnetic phase at zero magnetic field and temperatures above T_Q . Experimentally, (at zero temperature) additional reconstruction of the Fermi surface is observed above 2T. However, this unidentified phase above 2T is not connected to the phases observed at zero magnetic field and its explanation may require explicit inclusion of the magnetic field, which is beyond the scope of the current work. Our results expand on the previous toy model study demonstrating the possibility of two consecutive Kondo-destruction phase transitions [49]. Notice, however, that the previous toy model study did not identify the types of multipolar order, and also did not suggest the coexistence of quadrupolar with dipolar order in the fully Kondo-destroyed phase. We also discuss ultrasound measurements as an experimental probe of the multipolar susceptibilities at the different quantum critical points.

Here, we have solved a local version of the multipolar Kondo lattice model, but in future work it would be interesting to understand the full lattice problem with all the allowed multipolar moments, and determine whether quantum fluctuations beyond the local approximation are important or not. A further extension for our work is motivated by the fact that the phase transitions observed in experiments on $\text{Ce}_3\text{Pd}_{20}\text{Si}_6$ are tuned by the magnetic field [40,41]. Our model does not include the magnetic field explicitly, when in fact its effect on the Fermi surface, splitting of local moment states, and tetrahedral symmetry breaking nature may be important for connections with experiment. Another possible direction of theoretical inquiry is provided by the fact that when the Kondo effect is destroyed, not every moment that was initially hybridizing with the conduction electron becomes ordered. The remaining moments may enter a (potentially multipolar) spin liquid phase [69,70], with interactions mediated by the RKKY coupling providing a mechanism for frustration.

Although the construction of our model in the tetrahedral T_d environment was inspired by work on $\text{Ce}_3\text{Pd}_{20}(\text{Si, Ge})_6$, the results apply equally as well to other materials with a Γ_8 quartet in a cubic environment. This quartet can also arise in the presence of an octahedral O_h crystal field, as is the case for the ground state of Ce^{3+} in CeB_6 [36]. In fact, it is likely that such a rich phase diagram with possibility of both single- and two-stage Kondo destruction is the case in any rare-earth metallic system with a quartet of local mo-

ment ground states; this even applies to compounds with accidental fourfold degeneracy like YbRu_2Ge_2 [71,72]. This work therefore demonstrates the striking details one can uncover about exotic Kondo physics, the symmetries of multipolar ordering, and Fermi surface reconstruction based purely on local symmetry, and opens a new route to study novel quantum criticality in multipolar heavy fermion systems.

Acknowledgements. We thank S. Paschen and Q. Si for letting us know about their experimental and theoretical

works on Ce-based heavy fermion systems and for useful discussion. This work was supported by NSERC of Canada and the Center for Quantum Materials at the University of Toronto. This work was initiated at the Aspen Center for Physics, which is supported by National Science Foundation grant PHY-1607611. Y.B.K. is also supported by the Simons Fellowship from the Simons Foundation and the Guggenheim Fellowship from the John Simon Guggenheim Memorial Foundation. D.S. is supported by the Ontario Graduate Scholarship.

-
- [1] S. Doniach, *Physica B+C* **91**, 231 (1977).
 [2] P. Coleman, *Phys. Rev. B* **28**, 5255 (1983).
 [3] A. Schröder, G. Aeppli, R. Coldea, M. Adams, O. Stockert, H. Löhneysen, E. Bucher, R. Ramazashvili, and P. Coleman, *Nature (London)* **407**, 351 (2000).
 [4] P. Aynajian, E. H. Da Silva Neto, A. Gyenis, R. E. Baumbach, J. D. Thompson, Z. Fisk, E. D. Bauer, and A. Yazdani, *Nature (London)* **486**, 201 (2012).
 [5] Y. F. Yang, D. Pines, and G. Lonzarich, *Proc. Natl. Acad. Sci. USA* **114**, 6250 (2017).
 [6] A. Kumar, N. C. Hu, A. H. MacDonald, and A. C. Potter, *Phys. Rev. B* **106**, L041116 (2022).
 [7] Q. Si and F. Steglich, *Science* **329**, 1161 (2010).
 [8] N. Maksimovic, D. H. Eilbott, T. Cookmeyer, F. Wan, J. Ruzs, V. Nagarajan, S. C. Haley, E. Maniv, A. Gong, S. Faubel, I. M. Hayes, A. Bangura, J. Singleton, J. C. Palmstrom, L. Winter, R. McDonald, S. Jang, P. Ai, Y. Lin, S. Ciocys *et al.*, *Science* **375**, 76 (2022).
 [9] J. Prokleška, M. Kratochvílová, K. Uhlířová, V. Sechovský, and J. Custers, *Phys. Rev. B* **92**, 161114(R) (2015).
 [10] K. Inui and Y. Motome, *Phys. Rev. B* **102**, 155126 (2020).
 [11] G. Knebel, D. Aoki, and J. Flouquet, *C. R. Phys.* **12**, 542 (2011).
 [12] S. Seiro, L. Jiao, S. Kirchner, S. Hartmann, S. Friedemann, C. Krellner, C. Geibel, Q. Si, F. Steglich, and S. Wirth, *Nature Commun.* **9**, 3324 (2018).
 [13] H. Oh, S. Lee, Y. B. Kim, and E. G. Moon, *Phys. Rev. Lett.* **122**, 167201 (2019).
 [14] W. T. Fuhrman, A. Sidorenko, J. Hänel, H. Winkler, A. Prokofiev, J. A. Rodríguez-Rivera, Y. Qiu, P. Blaha, Q. Si, C. L. Broholm, and S. Paschen, *Sci. Adv.* **7**, eabf9134 (2021).
 [15] M. E. Sorensen and I. R. Fisher, *Phys. Rev. B* **103**, 155106 (2021).
 [16] P. Thalmeier, T. Takimoto, J. Chang, and I. Eremin, *J. Phys. Soc. Jpn.* **77**, 43 (2008).
 [17] A. Koitzsch, N. Heming, M. Knupfer, B. Büchner, P. Y. Portnichenko, A. V. Dukhnenko, N. Y. Shitsevalova, V. B. Filipov, L. L. Lev, V. N. Strocov, J. Ollivier, and D. S. Inosov, *Nature Commun.* **7**, 10876 (2016).
 [18] C. K. Barman, P. Singh, D. D. Johnson, and A. Alam, *Phys. Rev. Lett.* **122**, 076401 (2019).
 [19] P. Thalmeier, T. Takimoto, and H. Ikeda, *Philos. Mag.* **94**, 3863 (2014).
 [20] A. S. Patri, I. Khait, and Y. B. Kim, *Phys. Rev. Res.* **2**, 013257 (2020).
 [21] A. S. Patri and Y. B. Kim, *Phys. Rev. X* **10**, 041021 (2020).
 [22] D. J. Schultz, A. S. Patri, and Y. B. Kim, *Phys. Rev. Res.* **3**, 013189 (2021).
 [23] A. Sakai and S. Nakatsuji, *J. Phys. Soc. Jpn.* **80**, 063701 (2011).
 [24] P. Thalmeier, A. Akbari, and R. Shiina, *Rare-Earth Borides* **615** (2021).
 [25] K. Iwasa, T. Onimaru, T. Takabatake, R. Higashinaka, Y. Aoki, S. Ohira-Kawamura, and K. Nakajima, *Phys. B: Condens. Matter* **551**, 37 (2018).
 [26] A. S. Patri and Y. B. Kim, *SciPost Phys.* **12**, 057 (2022).
 [27] T. J. Sato, S. Ibuka, Y. Nambu, T. Yamazaki, T. Hong, A. Sakai, and S. Nakatsuji, *Phys. Rev. B* **86**, 184419 (2012).
 [28] M. Fu, A. Sakai, N. Sogabe, M. Tsujimoto, Y. Matsumoto, and S. Nakatsuji, *J. Phys. Soc. Jpn.* **89**, 013704 (2020).
 [29] Y. Shimura, Q. Zhang, B. Zeng, D. Rhodes, R. Schönemann, M. Tsujimoto, Y. Matsumoto, A. Sakai, T. Sakakibara, K. Araki, W. Zheng, Q. Zhou, L. Balicas, and S. Nakatsuji, *Phys. Rev. Lett.* **122**, 256601 (2019).
 [30] K. Matsubayashi, T. Tanaka, A. Sakai, S. Nakatsuji, Y. Kubo, and Y. Uwatoko, *Phys. Rev. Lett.* **109**, 187004 (2012).
 [31] M. Tsujimoto, Y. Matsumoto, T. Tomita, A. Sakai, and S. Nakatsuji, *Phys. Rev. Lett.* **113**, 267001 (2014).
 [32] A. Sakai, K. Kuga, and S. Nakatsuji, *J. Phys. Soc. Jpn.* **81**, 083702 (2012).
 [33] J. Kitagawa, N. Takeda, M. Ishikawa, T. Yoshida, A. Ishiguro, and T. Komatsubara, *Phys. B: Condens. Matter* **230–232**, 139 (1997).
 [34] T. Goto, T. Watanabe, S. Tsuduku, H. Kobayashi, Y. Nemoto, T. Yanagisawa, M. Akatsu, G. Ano, O. Suzuki, N. Takeda, A. Dönni, and H. Kitazawa, *J. Phys. Soc. Jpn.* **78**, 024716 (2009).
 [35] S. Paschen, S. Laumann, A. Prokofiev, A. M. Strydom, P. P. Deen, J. R. Stewart, K. Neumaier, A. Goukassov, and J. M. Mignot, *Phys. B: Condens. Matter* **403**, 1306 (2008).
 [36] R. Shiina, H. Shiba, and P. Thalmeier, *J. Phys. Soc. Jpn.* **66**, 1741 (1997).
 [37] A. M. Strydom, A. Pikul, F. Steglich, and S. Paschen, *J. Phys.: Conf. Ser.* **51**, 239 (2006).
 [38] H. Mitamura, T. Sakuraba, T. Tayama, T. Sakakibara, S. Tsuduku, G. Ano, I. Ishii, M. Akatsu, Y. Nemoto, T. Goto, A. Kikkawa, and H. Kitazawa, *J. Phys.: Conf. Ser.* **200**, 012118 (2010).
 [39] H. Ono, T. Nakano, N. Takeda, G. Ano, M. Akatsu, Y. Nemoto, T. Goto, A. Dönni, and H. Kitazawa, *J. Phys.: Condens. Matter* **25**, 126003 (2013).
 [40] V. Martelli, A. Cai, E. M. Nica, M. Taupin, A. Prokofiev, C. C. Liu, H. H. Lai, R. Yu, K. Ingersent, R. KÜchler, A. M. Strydom, D. Geiger, J. Haenel, J. Larrea, Q. Si, and S. Paschen, *Proc. Natl. Acad. Sci. USA* **116**, 17701 (2019).

- [41] F. Mazza, P. Y. Portnichenko, S. Avdoshenko, P. Steffens, M. Boehm, E. S. Choi, M. Nikolo, X. Yan, A. Prokofiev, S. Paschen, and D. S. Inosov, *Phys. Rev. B* **105**, 174429 (2022).
- [42] P. Coleman, C. Pépin, Q. Si, and R. Ramazashvili, *J. Phys.: Condens. Matter* **13**, R723 (2001).
- [43] Q. Si, S. Rabello, K. Ingersent, and J. L. Smith, *Nature (London)* **413**, 804 (2001).
- [44] S. Paschen, T. Lühmann, S. Wirth, P. Gegenwart, O. Trovarelli, C. Geibel, F. Steglich, P. Coleman, and Q. Si, *Nature (London)* **432**, 881 (2004).
- [45] F. Steglich, H. Pfau, S. Lausberg, S. Hamann, P. Sun, U. Stockert, M. Brando, S. Friedemann, C. Krellner, C. Geibel, S. Wirth, S. Kirchner, E. Abrahams, and Q. Si, *J. Phys. Soc. Jpn.* **83**, 061001 (2014).
- [46] J. Custers, K. A. Lorenzer, M. Müller, A. Prokofiev, A. Sidorenko, H. Winkler, A. M. Strydom, Y. Shimura, T. Sakakibara, R. Yu, Q. Si, and S. Paschen, *Nature Mater.* **11**, 189 (2012).
- [47] S. Friedemann, S. Wirth, N. Oeschler, C. Krellner, C. Geibel, F. Steglich, S. MaQuilon, Z. Fisk, S. Paschen, and G. Zwirgagl, *Phys. Rev. B* **82**, 035103 (2010).
- [48] S. Friedemann, N. Oeschler, S. Wirth, C. Krellner, C. Geibel, F. Steglich, S. Paschen, S. Kirchner, and Q. Si, *Proc. Natl. Acad. Sci. USA* **107**, 14547 (2010).
- [49] C.-C. Liu, S. Paschen, and Q. Si, *Proc. Natl. Acad. Sci. USA* **120**, e2300903120 (2023).
- [50] Q. Si and J. L. Smith, *Phys. Rev. Lett.* **77**, 3391 (1996).
- [51] J. L. Smith and Q. Si, *Europhys. Lett.* **45**, 228 (1999).
- [52] A. M. Sengupta, *Phys. Rev. B* **61**, 4041 (2000).
- [53] L. Zhu and Q. Si, *Phys. Rev. B* **66**, 024426 (2002).
- [54] G. Zaránd and E. Demler, *Phys. Rev. B* **66**, 024427 (2002).
- [55] S. Kirchner, L. Zhu, and Q. Si, *Phys. B: Condens. Matter* **359–361**, 83 (2005).
- [56] A. Dönni, T. Herrmannsdörfer, P. Fischer, L. Keller, F. Fauth, K. A. McEwen, T. Goto, and T. Komatsubara, *J. Phys.: Condens. Matter* **12**, 9441 (2000).
- [57] See Supplemental Material at <http://link.aps.org/supplemental/10.1103/PhysRevB.108.L060401> for the details, which includes Refs. [7,15,21,22,36,42–48,53,54,58–68].
- [58] J. P. Ellis, *Comput. Phys. Commun.* **210**, 103 (2017).
- [59] I. Affleck and A. W. Ludwig, *Nucl. Phys. B* **360**, 641 (1991).
- [60] I. Affleck and A. W. Ludwig, *Phys. Rev. B* **48**, 7297 (1993).
- [61] A. W. Ludwig and I. Affleck, *Phys. Rev. Lett.* **67**, 3160 (1991).
- [62] C. Mora, *Phys. Rev. B* **80**, 125304 (2009).
- [63] T. Kimura and S. Ozaki, *J. Phys. Soc. Jpn.* **86**, 084703 (2017).
- [64] D. J. Schultz, A. S. Patri, and Y. B. Kim, *Phys. Rev. B* **104**, 125144 (2021).
- [65] M. Lavagna, A. Jerez, and D. Bensimon, *Conc. Electron Correl.* **219** (2003).
- [66] D. Bensimon, A. Jerez, and M. Lavagna, *Phys. Rev. B* **73**, 224445 (2006).
- [67] S.E. Han, D. J. Schultz, and Y. B. Kim, *Phys. Rev. B* **106**, 155155 (2022).
- [68] A. S. Patri, A. Sakai, S. B. Lee, A. Paramekanti, S. Nakatsuji, and Y. B. Kim, *Nature Commun.* **10**, 4092 (2019).
- [69] T. Senthil, S. Sachdev, and M. Vojta, *Phys. Rev. Lett.* **90**, 216403 (2003).
- [70] T. Senthil, M. Vojta, and S. Sachdev, *Phys. Rev. B* **69**, 035111 (2004).
- [71] E. W. Rosenberg, J. H. Chu, J. P. Ruff, A. T. Hristov, and I. R. Fisher, *Proc. Natl. Acad. Sci. USA* **116**, 7232 (2019).
- [72] H. S. Jeevan, C. Geibel, and Z. Hossain, *Phys. Rev. B* **73**, 020407(R) (2006).